An Engineered Disulfide Bond between Residues 69 and 238 in Extended-Spectrum β-Lactamase Toho-1 Reduces Its Activity toward Third-Generation Cephalosporins‡

Akiko Shimizu-Ibuka,*,§ Hiroshi Matsuzawa,|| and Hiroshi Sakai§

Department of Food and Nutritional Sciences, University of Shizuoka, 52-1 Yada, Shizuoka 422-8526, Japan, and Department of Clinical Pharmacy, Faculty of Pharmaceutical Sciences, Aomori University, 2-3-1 Kohbata, Aomori 030-0943, Japan

Received July 15, 2004; Revised Manuscript Received September 29, 2004

ABSTRACT: Previous crystallographic structural analysis of extended-spectrum β-lactamase Toho-1 predicted that the high flexibility of β-strand B3, the region that contains a conserved KTG motif and forms one wall of the substrate-binding site, could be one of the key features contributing to Toho-1 activity toward third-generation cephalosporins. To investigate whether this possible flexibility really affects the substrate profile of this enzyme, two Toho-1 mutants have been produced, G238C and G238C/G239in, in which the glycine residue at position 238 was replaced with a cysteine and an additional glycine residue was inserted. Our intent was to introduce a disulfide bond between the cysteine residues at positions 69 and 238, and thus to lock the position of β-strand B3. The results of 5,5′-dithiobis(2-nitrobenzoic acid) (DTNB) titration indicated formation of a new disulfide bridge in the G238C mutant, although disulfide bond formation was not confirmed in the G238C/G239in mutant. Kinetic analysis showed that the activity of the G238C mutant decreased drastically against third-generation cephalosporins, while its catalytic efficiency against penicillins and first-generation cephalosporins was almost identical to that of the wild-type enzyme. This result was consistent with the prediction that flexibility in β-strand B3 was critical for activity against third-generation cephalosporins in Toho-1. Furthermore, we have determined the crystal structure of the G238C mutant enzyme to analyze the structural changes in detail. The structural model clearly shows the introduction of a new disulfide bridge and that there is no appreciable difference between the overall structures of the wild-type enzyme and the G238C mutant, although the introduced disulfide bond slightly influenced the positions of Ser237 on β-strand B3 and Asn170 on the Ω loop. The results of our kinetic and structural analyses suggest that the flexibility of β-strand B3, as well as the positions of Ser237 and the Ω loop, is critical for the substrate specificity expansion of Toho-1.

β-Lactamases, enzymes that confer bacterial resistance to β-lactam antibiotics, are organized in four classes (A−D), according to amino acid sequence and substrate specificity (*1*, *2*). Among them, class A β-lactamases are most frequently encountered in clinical isolates, often being encoded by genes located on transferable plasmids and exhibiting diverse substrate profiles (*3*). Class A enzymes were originally labeled as penicillinases on the basis of their substrate specificity. However, the number of class A enzymes with activity to hydrolyze expanded-spectrum cephalosporins has increased dramatically as the frequency of clinical use of new β-lactam antibiotics has increased (*2*, *3*). These enzymes with broad substrate specificity are known as extended-spectrum β-lactamases (ESBLs),[1] and they are further classified into several subgroups (*4*). The largest subgroup is that of non-ESBL derivatives, in which the extended-spectrum activity results from a few point mutations in the penicillinases such as TEM-1 and SHV-1 (*5*, *6*). The other subgroups consist of novel ESBLs distantly related to the previously identified class A β-lactamases (*6*). One subgroup includes a cluster of enzymes known as CTX-M-type β-lactamases, whereCTX refers to their powerful spectrum for hydrolysis of cefotaxime (*4*, *7*).

Toho-1 is a class A ESBL that is a member of the CTX-M subgroup based on its substrate profile and amino acid sequence. Previous structural analysis of Toho-1 noted that several features seemed to provide the activity toward third-generation β-lactams to this enzyme (*8*). One of these features was higher flexibility of β-strand B3, which contains a conserved KTG motif and forms one wall of the active site cleft. To investigate whether this possible flexibility really has any effect on the substrate specificity of Toho-1, we have produced two mutants, G238C and G238C/G239in. Our intent was to lock β-strand B3 into place by introduction of a new disulfide bridge between the cysteine residues at positions 69 and 238. In the G238C/G239in mutant, the

‡ The atomic coordinates of the Toho-1 G238C mutant have been deposited in the Protein Data Bank as entry 1WE4.

* To whom correspondence should be addressed at this address: Department of Applied Biological Chemistry, Graduate School of Agricultural and Life Sciences, The University of Tokyo, 1-1-1 Yayoi, Bunkyo-ku, Tokyo 113-8657, Japan. Phone: +81-3-5841-8117. Fax: +81-3-5841-8006. E-mail: aibuka@mail.ecc.u-tokyo.ac.jp or ibuka@u-shizuoka-ken.ac.jp.

§ University of Shizuoka.

|| Aomori University.

[1] Abbreviations: ESBL, extended-spectrum β-lactamase; IPTG, isopropyl α-D-thiogalactopyranoside; DTT, dithiothreitol; GuHCl, guanidine hydrochloride; DTNB, 5,5′-dithiobis(2-nitrobenzoic acid); rmsd, root-mean-square deviation; CD, circular dichroism; ND, not determined.

10.1021/bi048488u CCC: $27.50
Published on Web 11/24/2004

glycine residue at position 238 was replaced with a cysteine and an additional glycine residue was inserted at position 239. In designing this mutant, we referred to the amino acid sequences of class A enzymes with carbapenem-hydrolyzing activity, many of which are known to have a disulfide bridge between Cys69 and Cys238, though the role of the disulfide bond in their substrate specificity is still unclear (*9*−*13*). These mutants have been analyzed both kinetically and structurally, and the results suggest that the flexibility of β-strand B3, together with the positions of Ser237 and the Ω loop, is critical for the hydrolysis of the expanded-spectrum substrates.

MATERIALS AND METHODS

Bacterial Strains and Plasmids. Escherichia coli strains CJ236 [*dut*1 *ung*1 *thi*-1 *relA*1/*pCJ*105(F′ *cam*^{r})], MV1184 [*ara*, Δ(*lac-pro*AB), *rpsL*, *thi* (ϕ80 *lacZ* ΔM15), Δ(*srl-rec*A)-306::Tn*10*(*tet*^{r})/F′[*traD*36, *proAB*$^+$, *lac* I ^{q}, *lacZ*Δ*M*15]], and BL21(DE3)pLysS [F$^-$ *dcm ompT hsd*S$_B$ ($r_B^-m_B^-$) *gal* λ(DE3) pLysS(Cam^r)] were used for site-directed mutagenesis, subsequent genetic constructions, and overproductions of proteins, respectively. The Toho-1 gene was cloned and sequenced as described previously (*14*). A previously constructed plasmid, pET-bla, was used for the overexpression of wild-type Toho-1 (*15*).

Site-Directed Mutagenesis. The mutants were constructed by site-directed mutagenesis using the Kunkel method with the MUTA-GENE in vitro mutagenesis kit (Bio-Rad, Carlsbad, CA) (*16*). For mutagenesis, the pre119PA plasmid, in which the gene encoding the wild-type Toho-1 enzyme was digested with the restriction enzymes *Bam*HI and *Sac*I and inserted into the multiple cloning region of pUC119 in the reverse direction, was used. The oligonucleotide primer 5′-GAT AAA ACC GGA TCC TGT GAT TAT GGC ACC ACC AAC-3′ was synthesized for the G238C mutation, and the primer 5′-GAT AAA ACC GGC AGC TGT GGA GAT TAT GGC ACC ACC-3′ was used for the G238C/G239in mutation. The nucleotide sequence of each mutant was confirmed by DNA sequencing with a Taq Dye Deoxy Terminator Cycle Sequencing Kit and a model 373A DNA sequencer (Applied Biosystems Inc.). The mutated genes were isolated by digestion with the restriction enzymes *Bst*XI and *Eco*RV, and were inserted into plasmid vector pET-bla, which was digested with the same enzymes to yield pET-G238C and pET-G238C/G239in. These were used for overexpression of G238C and G238C/G239in, respectively.

Expression and Purification of the Protein. The expression and purification of the wild-type and mutant enzymes were performed according to procedures described previously (*15*). Briefly, the plasmids constructed for the expression of enzymes were transformed into *E. coli* BL21(DE3)pLysS, and protein production was performed in 100 mL of 2-TY broth supplemented with 50 μg/mL kanamycin. For the G238C/G239in mutant, protein was produced in 500 mL of 2-TY broth because of a low production level. The cells were grown at 30 °C for 8 h, and protein production was induced by addition of 0.1 mM IPTG when the absorbance of the cell culture at 600 nm was around 0.5. The cells were harvested by centrifugation, dissolved in 10−15 mL of 20 mM MES buffer (pH 6.5), and then disrupted by sonication. After centrifugation, the enzyme in the supernatant was purified by ion exchange chromatography on a CM-Toyopearl column (Tosoh) in 20 mM MES buffer (pH 6.5), and then was eluted with a 0 to 0.15 M NaCl linear gradient. The purity of the enzyme was assessed to be more than 95% by Coomassie blue staining after SDS−polyacrylamide gel electrophoresis.

Thiol Titration with DTNB. The free thiol content was analyzed by reaction with DTNB ($\Delta\epsilon_{412}$ = 13 700 M^{-1} cm^{-1}) (*17*). Each of the wild-type and mutant Toho-1 enzyme solutions was prepared either under native conditions in 0.1 M Tris-HCl (pH 8.0) or under a denatured and reduced condition in 0.1 M Tris-HCl (pH 8.0) containing 6 M GuHCl and 25 mM DTT. All of the fractions were incubated at 25 °C for 1 h. The buffer was then exchanged with 0.1 M sodium acetate (pH 5.5) using a Microcon 10 concentrator (Amicon) to remove excess DTT. The volume of each 50 μL sample was increased to 500 μL to contain 0.1 M sodium phosphate buffer (pH 7.3), 6 M GuHCl, and 1 mM EDTA; 25 μL of 3 mM DTNB in 0.1 M sodium phosphate buffer (pH 7.3) was added to each sample, and the absorbance at 412 nm was measured at 25 °C.

Circular Dichroism (CD) Spectroscopy. The CD spectra were measured with a J720 spectropolarimeter (Jasco, Tokyo, Japan) equipped with a thermoelectric temperature control. Solutions with a protein concentration of 0.10−0.20 mg/mL in 5 mM sodium phosphate buffer (pH 7.0) were placed in 1 mm quartz cuvettes for far-UV experiments (wavelengths of 185−250 nm). The spectra were recorded every 0.1 nm with scan rate of 20 nm/min at 25 °C, and averaged over four runs. After buffer baseline subtraction, the CD data were normalized to protein concentration and are expressed as molar residue ellipticity. Thermal unfolding transitions were monitored by measuring the CD signal at 222 nm at different temperatures (20−90 °C) with a heating rate of 0.8 °C/min. The raw data were normalized to sample concentrations and corrected for pre- and post-transition slopes.

Kinetic Assays. The following antibiotics and chemicals were used for kinetic assays. Ampicillin ($\Delta\epsilon_{235}$ = −900 M^{-1} cm^{-1}) and cefotaxime ($\Delta\epsilon_{264}$ = −7250 M^{-1} cm^{-1}) were purchased from Wako Chemicals (Tokyo, Japan). Benzylpenicillin ($\Delta\epsilon_{233}$ = −1140 M^{-1} cm^{-1}), cephalothin ($\Delta\epsilon_{262}$ = −7660 M^{-1} cm^{-1}), cephaloridine ($\Delta\epsilon_{260}$ = −10200 M^{-1} cm^{-1}), ceftazidime ($\Delta\epsilon_{265}$ = −10300 M^{-1} cm^{-1}), and aztreonam ($\Delta\epsilon_{318}$ = −650 M^{-1} cm^{-1}) were purchased from Sigma Chemical Co. (St. Louis, MO). Nitrocefin ($\Delta\epsilon_{482}$ = 15000 M^{-1} cm^{-1}) was purchased from Unipath Oxoid (Basingstoke, United Kingdom). Cefuzoname ($\Delta\epsilon_{275}$ = 7950 M^{-1} cm^{-1}) was from Lederle Japan Ltd. (Tokyo, Japan). Imipenem ($\Delta\epsilon_{278}$ = −5660 M^{-1} cm^{-1}) was from Banyu Pharmaceutical Co. Ltd. (Tokyo, Japan). Hydrolysis of β-lactam antibiotics was detected by monitoring the variation in the absorbance of the β-lactam solution in 50 mM phosphate buffer (pH 7.5). All the measurements were taken on a JASCO V-530 spectrophotometer linked to a personal computer. The reaction was performed in a total volume of 500 μL at 30 °C. For dilution of the enzyme, BSA was added to the buffer to a final concentration of 20 μg/mL to prevent denaturation of the enzyme. The progress curves were measured at least three times for each substrate, and reproducible results were obtained. The K_i for imipenem was determined using 300 μM nitrocefin as a reporter substrate.

Table 1: Data Collection and Processing[a]

wavelength (Å)	1.0
temperature (K)	100.0
space group	$P3_221$
unit cell (Å)	$a = b = 72.7$, $c = 98.3$
resolution range (Å)	24.5−1.70 (1.79−1.70)
no. of observations	705402 (52386)
no. of unique reflections	33629 (4813)
completeness (%)	100.0 (100.0)
average $I/\sigma(I)$	10.9 (4.3)
R_{merge}[b] (%)	4.9 (17.2)

[a] Values in parentheses refer to the highest-resolution shell. [b] $R_{merge} = \sum_i |I_{av} - I_i| / \sum_i |I_i|$, where I_{av} is the average of all individual observations I_i.

Precise description of the analysis was published previously (*15*, *18*).

Crystal Preparation and Data Collection. The purified protein was dialyzed against 5 mM Tris-HCl buffer (pH 7.0) and concentrated to 10 mg/mL for crystallization. The crystals were prepared by the hanging drop or sitting drop vapor diffusion method with reservoir solutions of 1.8−2.0 M ammonium sulfate in 100 mM sodium acetate buffer (pH 4.5−4.6) at 15−20 °C. Thin hexagonal-shaped crystals suitable for X-ray analysis were obtained within ∼1 month. X-ray diffraction data were collected at Station BL6A of the Photon Factory, the High Energy Accelerator Research Organization (KEK, Tsukuba, Japan), at 100 K with a Mar charge-coupled device (CCD) detector. The crystals were cryoprotected in a solution of 30% sucrose and 2.6 M ammonium sulfate and then flash-frozen in liquid nitrogen. The reflection was indexed, integrated, and scaled using the DPS/Mosflm software package (*19*, *20*). The space group was determined to be $P3_221$ with one protein molecule per asymmetric unit and the following unit cell dimensions: $a = b = 72.7$ Å and $c = 98.3$ Å. The statistics are summarized in Table 1.

Structure Determination. The refinement was performed using data for which $F > 0\sigma(F)$ to 1.70 Å. The initial model for refinement was the structure of the Toho-1 E166A mutant (PDB entry 1BZA) (*8*). The model was subjected to rigid body refinement, followed by a simulated annealing protocol with an initial temperature of 2000 K, positional minimization, and individual *B* factor refinement using CNS (*21*). Manual model building was performed with O (*22*). The stereochemical quality of the model was monitored periodically using Procheck (*23*). After the protein structure had been modeled, water molecules were automatically picked out using CCP4 (*24*). Sulfate ions were modeled into the obvious tetrahedral-shaped electron density in the solvent.

RESULTS

Construction, Expression, and Purification of Mutant Toho-1 Enzymes. Partial sequence alignment of Toho-1 and several other class A β-lactamases is shown in Figure 1. The amino acid numbering used in this study follows the consensus numbering of Ambler et al. (*2*), and the secondary structural elements were labeled according to the notations used for the wild-type and E166A Toho-1 enzyme (*8*, *15*). Two Toho-1 mutants, G238C and G238C/G239in, were constructed to introduce a disulfide bond between the residues at positions 69 and 238 in Toho-1. G238C was designed simply by referencing the crystal structure of Toho-1. G238C/G239in, in which a glycine residue at position 238 was replaced with a cysteine and an additional glycine residue was inserted, was designed on the basis of the amino acid sequences of class A carbapenemases such as Sme-1 and NMC-A. These enzymes have a disulfide bond between Cys69 and Cys238 (Figure 1) (*9*−*13*). The Toho-1 mutants were expressed and purified in the same manner as the wild-type enzyme. The expression level of G238C/G239in in *E. coli* BL21(DE3)pLysS was approximately one-tenth of that of wild-type Toho-1, while G238C was expressed at a level similar to that of the wild-type enzyme (data not shown).

Disulfide Bond Formation in the Mutants. Free thiol groups in the enzymes were titrated with DTNB to analyze disulfide bond formation in the Toho-1 enzymes (Table 2). Since the wild-type enzyme has only one cysteine residue at position 69, the number of free SH groups per mutant molecule should be zero if the S−S bridge is formed, or two if no disulfide bond formation occurs. In G238C, the number of free SH groups per molecule was estimated to be 0.1 in the absence of DTT, and 1.8 in the presence of both DTT and GuHCl. This result confirmed the formation of a disulfide bridge in the G238C mutant. For the G238C/G239in mutant, the number of free SH groups per molecule was determined to be 1.4 in the absence of DTT. This indicated that no disulfide bond was formed in this mutant, at least in the majority of the molecules.

Effect of the Mutations on Secondary Structure and Thermal Stability. The far-UV CD spectra of the enzymes were superimposable, indicating that the mutations did not induce significant changes in the secondary structural elements in both G238C and G238C/G239in (Figure 2a). The thermal unfolding curves are shown in Figure 2b. The wild-type enzyme and G238C exhibited cooperative unfolding behavior, while G238C/G239in exhibited a relatively gradual decrease in molar residue ellipticity. The melting temperatures (T_m) derived from the analysis of the CD melting curve were 52.2 ± 0.8, 60.9 ± 0.5, and 50.9 ± 1.1 °C for the wild-type enzyme, the G238C mutant, and the G238C/G239in mutant, respectively (Figure 2b). The result of irreversible heat inactivation analysis, which was monitored by the remaining activity against nitrocefin after incubation of enzyme solutions at various temperatures, also indicated higher stability of the G238C mutant (data not shown).

Kinetic Study. The steady-state kinetic parameters k_{cat} and K_m for several β-lactam substrates are summarized in Table 3. Two mutants exhibited kinetic properties that were obviously different, and that also differed from those of the wild-type enzyme. For the G238C mutant, all the determined k_{cat} and K_m values were smaller than the corresponding values of the wild-type enzyme. In the hydrolysis of penicillins and first-generation cephalosporins, the decrease in k_{cat} was balanced by a reduction in K_m so that k_{cat}/K_m values only decreased slightly in the range of 82−86% of the corresponding values for wild-type Toho-1. In contrast, k_{cat}/K_m for third-generation cephalosporins decreased drastically to the level of 0.043−21%, due to a substantial decrease in k_{cat}. In the G238C/G239in mutant, K_m values tended to increase and k_{cat} values to decrease for all of the substrates except aztreaonam. The increase in K_m values was more significant for penicillins, and the decrease in k_{cat} was more considerable for cerphalosporins. As a consequence, k_{cat}/K_m decreased for all of the substrates, in the range of 14−22%

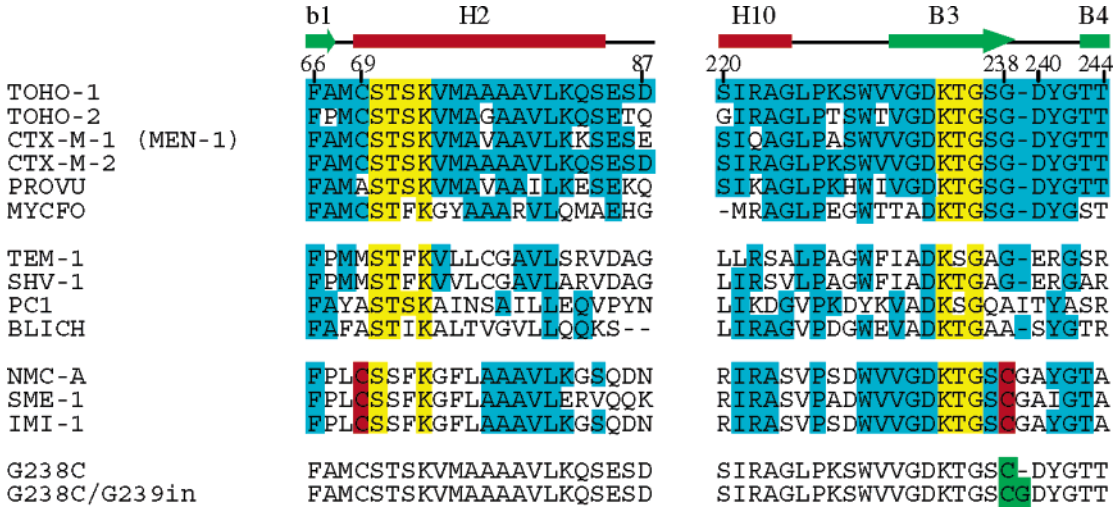

FIGURE 1: Partial sequence alignment of Toho-1 and class A β-lactamases. Aligned enzymes are Toho-1, Toho-2, CTX-M-1 (also known as MEN-1), CTX-M-2, the β-lactamase from *P. vulgaris* K1 (PROVU) and *Mycobacterium fortuitum* (MYCFO), TEM-1, SHV-1, the β-lactamase from *S. aureus* PC1 (PC1) and *Bacillus licheniformis* 749/C (BLICH), NMC-A, Sme-1, and IMI-1. The five β-lactamases listed directly below Toho-1 are ESBLs; the next four are non-ESBLs, and the following three are the enzymes known as carbapenemases. The two enzymes at the bottom are the Toho-1 mutants constructed in this study. The secondary structure elements are shown at the top, with green arrows representing β-strands and red rods representing α-helices. The residues included in the three conserved regions of class A β-lactamases are highlighted in yellow, while the residues identical to the corresponding ones in Toho-1 are highlighted in cyan. The cysteine residues that form a disulfide bond in the carbapenemases are highlighted in red, and the residues that were replaced in the Toho-1 mutants are highlighted in green.

Table 2: Number of Free Thiol Groups in the Wild-Type and Mutant Toho-1 Enzymes

enzyme	condition	SH per enzyme
wild-type	native	0.8 ± 0.1
	GuHCl- and DTT-treated	1.0 ± 0.1
G238C	native	0.1 ± 0.0
	GuHCl- and DTT-treated	1.8 ± 0.2
G238C/G239in	native	1.4 ± 0.3
	GuHCl- and DTT-treated	1.6 ± 0.2

for penicillins and first-generation cephalosporins, and in the range of 0.024−2.4% for third-generation cephalosporins. For both mutants, a large decrease in activity against ceftazidime, which was a poor substrate for wild-type Toho-1, was observed. In the case of aztreonam, the decrease in both k_{cat} and K_m was extreme in both mutants, especially in G238C/G239in. Moreover, the Toho-1 mutants did not acquire significant hydrolytic activity against carbapenems (data not shown).

Since G238C had a disulfide bond and exhibited a selective decrease of activity against third-generation cephalosporins, we measured its K_i for imipenem to further analyze the kinetic properties of this mutant. The result showed that the K_i of G238C for imipenem was 1/18 of that of the wild-type enzyme, indicating that G238C became much more sensitive to imipenem than wild-type Toho-1 (Table 3).

Crystal Structure of G238C. To obtain precise information about structural changes in the G238C mutant, this enzyme has been analyzed by X-ray crystallography. The refined structure of the G238C mutant is well-defined except for the N-terminal methionine at position 26, which was inserted for overexpression. The model includes 261 amino acid residues, 344 water molecules, and seven sulfate ions. The final model was refined to an R factor of 18.3% and an R_{free} of 20.0% at 1.70 Å resolution. The refinement results are summarized in Table 4. Alternative conformations were assigned to the side chains of the residues at positions 96, 146, 186, 201, 218, and 278. Glu96, Asp146, and Glu201 are on the protein surface of the α domain, far from the active site. Met186 is at the interface of the two domains, and is a constituent residue of the "hydrophobic core" that is conserved in the enzymes of the CTX-M family (*8*). Ser218 is positioned on the top edge of the active site cleft. Ile278 is on α-helix H11 of the α/β domain, and is positioned in the vicinity of hydrophobic residues such as Arg275 and Phe265, where it is half-buried between α-helices H11 and H1. An alternative conformation of Lys73, which has been assigned in the wild-type Toho-1 enzyme, was not observed in the G238C structure. In the G238C mutant, the Lys73 side chain is pointed toward the carboxyl group of Glu166.

The structure of the G238C mutant clearly shows the existence of the engineered disulfide bridge between Cys69 and Cys238 (Figure 3a). The introduction of the disulfide bond has not altered the architecture of this enzyme as a whole, and the active site structure of the G238C mutant is almost identical to that of the wild-type enzyme (Figure 3b). When the coordinates of the two models are superimposed, the rmsd value is 0.122 Å for Cα atoms and 0.241 Å for all atoms. However, the slight changes are localized near the disulfide bridge. The differences in Cα positions corresponding to residues Cys69 and Cys238, the residues directly involved in formation of the new disulfide bond, are 0.36 and 0.31 Å, respectively. The positions of the residues neighboring Cys69, such as Ala67, Met68, and Ser70, are not significantly affected by the introduction of the disulfide bond, with changes in Cα positions of 0.08, 0.20, and 0.16 Å, respectively. The positions of the residues on β-strand B3 are influenced more by the new disulfide bridge. In particular, the positional differences in the Ser237 atoms are larger than those of the Cys238 Cα atom, with the positional differences in Cα, Oγ, and main chain N, C, and O atoms of 0.43, 0.50, 0.41, 0.51, and 0.80 Å, respectively. Moreover, the position of Asn170 on the Ω loop is also affected, with a shift in the Cα atom of 0.37 Å. As a result of these changes,

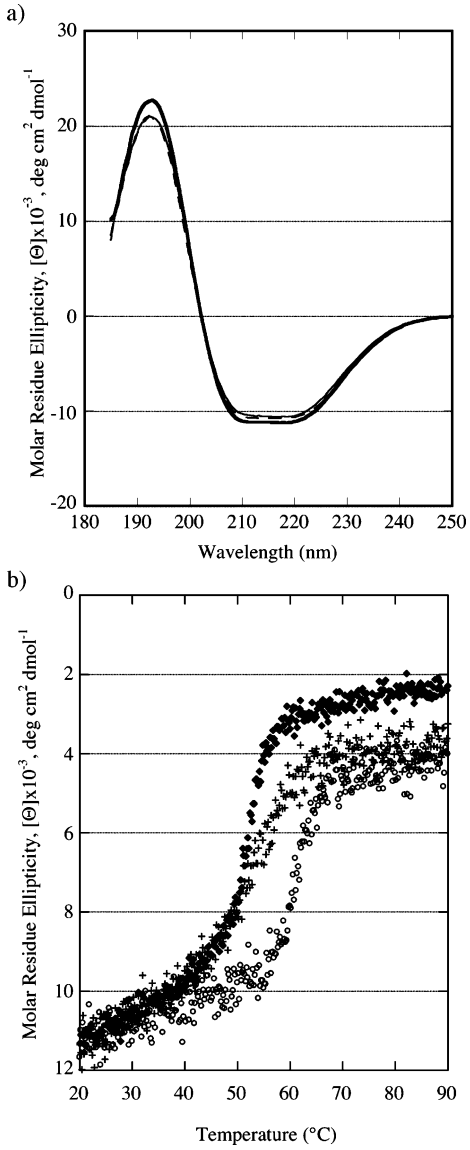

FIGURE 2: Secondary structure and thermal stability of Toho-1 enzymes. (a) Far-UV CD spectra at pH 7.0 and 25 °C. The spectra of the wild-type enzyme (thick solid line), G238C (thin solid line), and G238C/G239in (dotted line) are shown. (b) Heat of unfolding of Toho-1 enzymes monitored by CD at 222 nm: (◆) wild type, (○) G238C, and (+) G238C/G239in.

the Ω loop has become slightly more distant from β-strand B3, and the distance between the Cys238 Cα atom and the Asn170 Cα atom becomes larger than the corresponding distance in the wild-type enzyme by 0.47 Å (Figure 3c).

There is no significant difference in the disposition of water molecules in the active site between the G238C mutant and the wild-type enzyme (Figure 3b). Water molecules Wat36 and Wat30 are in the positions corresponding to Wat41 and Wat49 of the wild-type enzyme and Wat81 and Wat22 of *Staphylococcus aureus* PC1 β-lactamase (PDB entry 3BLM), respectively (*25*). Wat36 is hydrogen-bonded to Ser70 N, Ser70 Oγ, and Asn170 Nδ2, and it is regarded as a hydrolytic water that is essential for deacylation. Wat30 is hydrogen-bonded to Ser237 N, Ser70 N, and Ser70 Oγ, and it corresponds to the water molecule normally found in the oxyanion hole (*25*). Two water molecules, Wat36 and Wat55, are located in positions close to the carboxyl group of Glu166 at distances from Glu166 Oϵ1 of 2.75 and 2.63 Å, respectively. However, no hydrogen bonds are formed between Glu166 and these water molecules in both the G238C mutant and the wild-type enzyme. Moreover, no difference can be observed in the hydrogen bonding network at the active site between the wild-type enzyme and the G238C mutant. A hydrogen bond between the CO group at position 170 on the Ω loop and the NH group at position 240 on β-strand B3 is conserved in both the wild-type enzyme and the G238C mutant, at distances of 3.02 and 3.21 Å, respectively.

DISCUSSION

Formation of a Disulfide Bridge. We intended to lock β-strand B3 into place by introducing a disulfide bridge between the residues at positions 69 and 238. In the case of the G238C mutant, the expected disulfide bond formation was verified by both titration with DTNB and X-ray analysis, and it resulted in a T_m value higher than that of the wild-type enzyme by 8.7 °C. However, formation of the disulfide bridge was not confirmed in the G238C/G239in mutant. In the G238C/G239in mutant, the number of free SH groups per molecule was 1.4 in the absence of DTT (Table 2), which was closer to 2 than to 0, indicating that most of the SH groups were in fact free. Interestingly, the addition of 10 mM DTT decreased the activity of G238C/G239in for nitrocefin to 20% of the activity measured without DTT, whereas this phenomenon was observed for neither the wild type nor the G238C enzyme (data not shown). From these results, we speculate that most of the total G238C/G239in activity might be due to the small population of G238C/G239in molecules in which an S−S bond was formed, and the reduction of this disulfide bond could be responsible for the loss of activity. It was also observed that the production level of this mutant was much lower than that of the wild-type and G238C enzymes. Though CD spectra showed that there was no detectable change in the secondary structure (Figure 2a), and therefore probably no drastic change in the overall structure of the G238C/G239in mutant, the mutation might have made the protein unstable and/or partially disordered.

Substrate Profile of the Toho-1 Mutants. The most striking change in the catalytic property of the G238C mutant was the limited decrease in k_{cat} and k_{cat}/K_m for third-generation cephalosporins and aztreonam. In the previous study of Toho-1, we suggested that the flexibility of β-strand B3 might have been critical in Toho-1 for the hydrolysis of third-generation cephalosporins (*8*). The results of kinetic analyses of the G238C mutant were consistent with this prediction that the loss of flexibility at β-strand B3 narrowed the substrate specificity of Toho-1.

It was also intriguing that both k_{cat} and K_m values for all the substrates that were tested decreased in the G238C mutant. Similar kinetic changes were observed in the studies of the G238S mutants of the SHV-1 and TEM-1 β-lactamases (*26*, *27*). These studies suggested that the side chains larger than alanine at position 238 crowded against the side chains of residues 67, 69, and 170 to push the lower part of β-strand B3 away from the active site, giving more space for β-lactam side chains to bind the active site pocket, and thus lowering the K_m values. It is proposed that at the same time, the G238S mutation causes the β-lactam ring to be held slightly farther

Table 3: Kinetic Parameters of Toho-1 against Various Antibiotics

class (generation)[a]	antibiotic	wild type			G238C			G238C/G239in		
		k_{cat} (s^{-1})	K_m (μM)	k_{cat}/K_m ($\mu M^{-1} s^{-1}$)	k_{cat} (s^{-1})	K_m (μM)	k_{cat}/K_m ($\mu M^{-1} s^{-1}$)	k_{cat} (s^{-1})	K_m (μM)	k_{cat}/K_m ($\mu M^{-1} s^{-1}$)
penicillins	ampicillin	41 ± 2	22 ± 4	1.9	29 ± 1	18 ± 2	1.6	18 ± 4	42 ± 7	0.43
	penicillin G	63 ± 4	17 ± 2	3.7	18 ± 1	5.7 ± 1.5	3.2	20 ± 1	41 ± 3	0.49
cephalosporins (I)	cephalothin	760 ± 13	178 ± 3	4.30	88.3 ± 4.0	23.4 ± 1.2	3.77	163 ± 12	217 ± 9	0.751
	cephaloridine	281 ± 9	264 ± 7	1.06	51.5 ± 3.2	56.9 ± 1.0	0.905	38.2 ± 1.4	258 ± 7	0.148
cephalosporins (III)	cefotaxime	ND	ND[b]	1.59 ± 0.53	29.8 ± 1.1	118 ± 3	0.253	7.06 ± 0.59	183 ± 12	0.0386
	cefuzoname	520 ± 17	176 ± 5	2.95	84.3 ± 2.9	135 ± 7	0.624	ND	ND[b]	$(499 \pm 11) \times 10^{-4}$
	ceftazidime	ND	ND[b]	1.58 ± 0.02	ND	ND[b]	$(676 \pm 15) \times 10^{-6}$	ND	ND[b]	$(377 \pm 16) \times 10^{-6}$
monobactam	aztreonam	7.3 ± 0.8	36 ± 6	0.20	0.63 ± 0.11	7.6 ± 0.7	0.080	$(76 \pm 2) \times 10^{-3}$	ND[c]	ND
carbapenem	imipenem	ND	$(36 \pm 4) \times 10^{-3}$ [d]	ND	ND	$(19 \pm 3) \times 10^{-4}$ [d]	ND			

[a] Generation of cephalosporins is indicated in parentheses. [b] Too large to determine. [c] Too small to determine. [d] K_i value determined by substrate competition experiments with nitrocefin.

Table 4: Refinement Statistics[a]

resolution range (Å^2)	20−1.70 (1.78−1.70)
R factor[b] (%)	18.3 (22.2)
R_{free}[c] (%)	20.0 (23.8)
average B factor (Å^2)	
whole structure	15.5
main chain	12.1
side chain	14.9
solvent	27.6
rmsd from ideal values	
bonds (Å)	0.004
angles (deg)	1.40
Ramachandran analysis[d] (%)	
most favored	91.4 (212)[e]
additional allowed	8.2 (19)[e]
generously allowed	0.4 (1)[e]
disallowed	0 (0)[e]

[a] Values in parentheses refer to the highest-resolution shell. [b] $R = \sum|F_o - F_c|/\sum|F_o|$, where F_o and F_c are the observed and calculated structure factor amplitudes, respectively. [c] $R_{free} = \sum|F_o - F_c|/\sum|F_o|$, calculated using a test data set consisting of 10% of the total data randomly selected from the observed reflections. [d] Ramachandran analysis was carried out using Procheck (*23*). [e] Values in parentheses are the numbers of non-glycine and non-proline residues in each region.

from the nucleophilic oxygen atom of Ser70, thus resulting in a decreased k_{cat} (*26*, *27*). We suspect that an analogous change has occurred in the G238C mutant of Toho-1, and this is actually seen in the crystal structure of the G238C enzyme, as mentioned below. A good alternative possibility is that the reduced elasticity at the substrate-binding site resulting from introduction of the disulfide bridge might cause more stable binding of substrates, as well as structural restraints, which could prevent active site components from making appropriate motions that are necessary for catalysis, resulting in the reduction of both K_m and k_{cat}. In such a case, a simultaneous decrease in k_{cat} and K_m might be explained by a decrease in k_{+3}.

The G238C mutant was found to be much more sensitive to imipenem than the wild-type enzyme was. It has been suggested that strong inhibition of class A β-lactamase by imipenem is caused by the interaction between Asn132 of the enzyme and the C6α hydroxyethyl group of imipenem, which prevents deacylation of imipenem (*28*). We suppose therefore that this interaction becomes more stabilized by introduction of the disulfide bridge in the Toho-1 G238C mutant.

As for the G238C/G239in mutant, the hydrolytic activity decreased significantly for all of the tested substrates. This indicated that the insertion of a glycine residue at position 239 prevented the enzyme from becoming fully active, possibly by making the active site structure somewhat loose or disordered, as mentioned above. Possibly, as seen in the structure of *S. aureus* PC1 β-lactamase, the backbone of the residue inserted at position 239 might protrude into the substrate binding site, causing the decrease in hydrolytic activity (*29*). The decrease in activity was more drastic for expanded-spectrum substrates, clearly indicating that the mutated region was more critical for the hydrolysis of these substrates than for penicillins and first-generation cephalosporins. These results were consistent with previous studies of Toho-1 and other class A β-lactamases, which suggested that the C-terminal side of β-strand B3 was important for the expansion of substrate specificity (*8*, *26*, *27*, *29*, *30*).

Structural Change in the G238C Mutant and Its Correlation with Altered Kinetic Properties. The crystal structure shows that the introduction of a disulfide bond between residues 69 and 238 does not cause a considerable change in the overall structure. This result, taken together with the kinetic analysis, seems to support the prediction that indeed the "flexibility" of β-strand B3 is important for efficient catalytic activity against third-generation cephalosporins. Yet, it should be noted that the positional changes of Ser237 on β-strand B3 and of Asn170 on the Ω loop are subtle, but are still significantly larger than those of other residues in the vicinity of the disulfide bridge. In studies of Toho-1 and several class A β-lactamases, it has been suggested that β-strand B3 and/or the Ω loop is deeply involved in the substrate specificity expansion of the enzymes (*31*−*34*). Therefore, we cannot neglect the possibility that these positional changes observed in the G238C crystal structure altered the kinetic properties of the G238C mutant. Kinetic and structural studies of several class A ESBLs indicated that Ser237, the residue conserved in the CTX-M-type and some other ESBLs (Figure 1), was critical for the hydrolysis of expanded-spectrum substrates (*31*, *35*−*38*). *Proteus vulgaris* K1 β-lactamase, which is also an ESBL and whose sequence is 71% identical with that of Toho-1 and possesses a serine residue at position 237, has been well studied both structurally and kinetically (*35*, *36*). Ser237Ala mutations

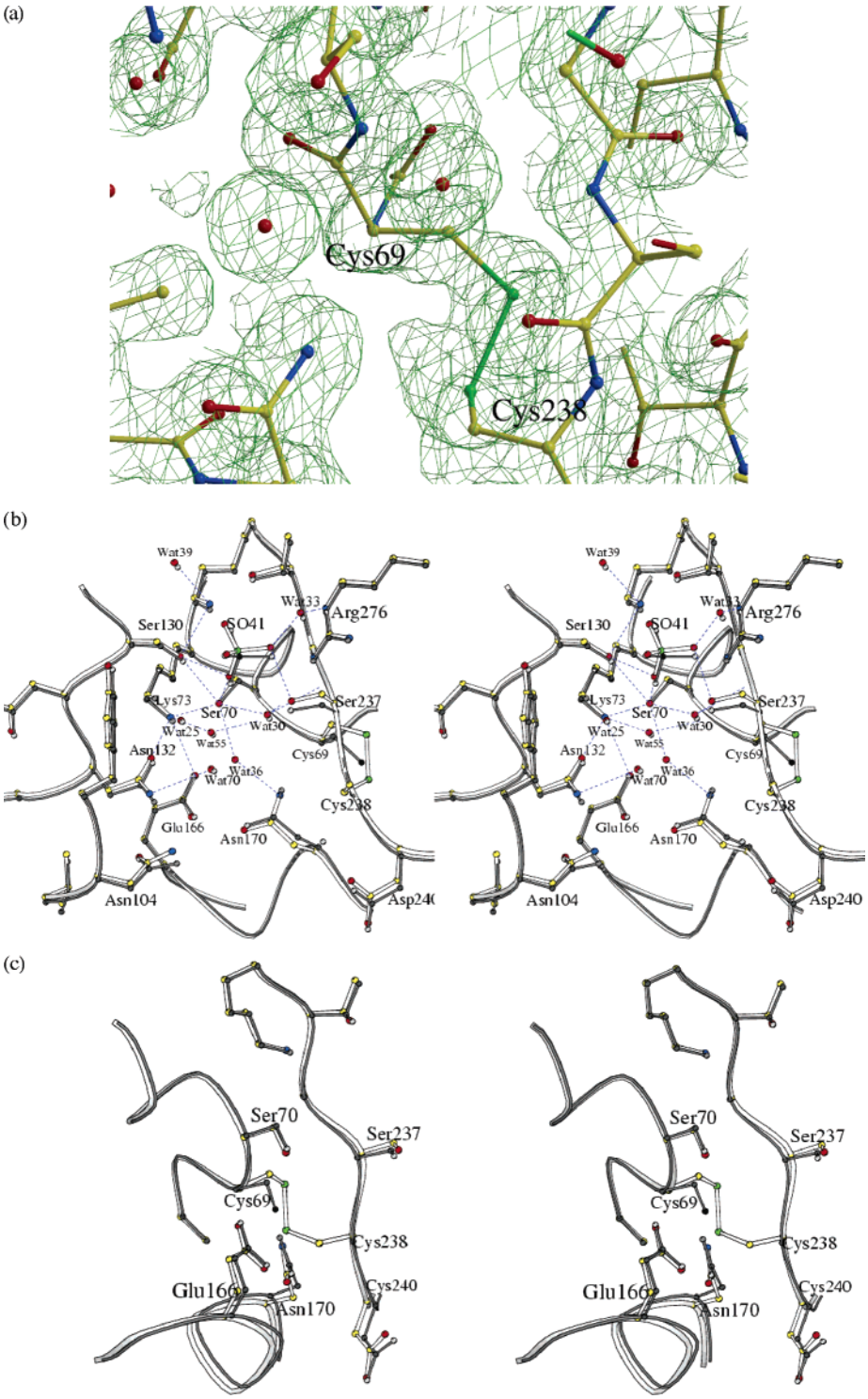

FIGURE 3: Active site structure of the G238C mutant. (a) Electron density map in the vicinity of the disulfide bridge introduced between Cys69 and Cys238. (b) Superposition of the wild-type and G238C structures at the active site. (c) Superposition of the wild type and G238C mutant around β-strand B3 and the Ω loop. In both panels b and c, the wild-type enzyme is colored gray and the G238C mutant white. Atoms are shown with CPK color, and hydrogen bonds are indicated. These figures were drawn with O (*22*), Molscript (*40*), Bobscript (*41*), and Raster3D (*42*, *43*).

were generated in the *P. vulgaris* K1 enzyme and CTX-M-4, and their activity against oxyimino cephalosporins fell significantly, mainly due to a decrease in k_{cat} (*35*, *38*). Since the G238C mutant of Toho-1 exhibited similar changes in its kinetic characteristics, there is a possibility that the introduced S−S bond prevented Ser237 from properly interacting with third-generation cephalosporins, by slightly changing its position or by limiting the motion of Ser237. It has also been reported that the Ser237Ala mutant of carbapenemase Sme-1 decreases its activity against imipenem to $^1/_5$ of that of the wild-type Sme-1 enzyme (*37*). The Sme-1 structure shows that the hydroxyl group of Ser237 is stabilized by two hydrogen bonds with the guanidium group of Arg220, and that the main chain NH group of Ser237 contributes to the oxyanion hole (*11*). Since there is no arginine residue at position 220 in Toho-1, this mechanism

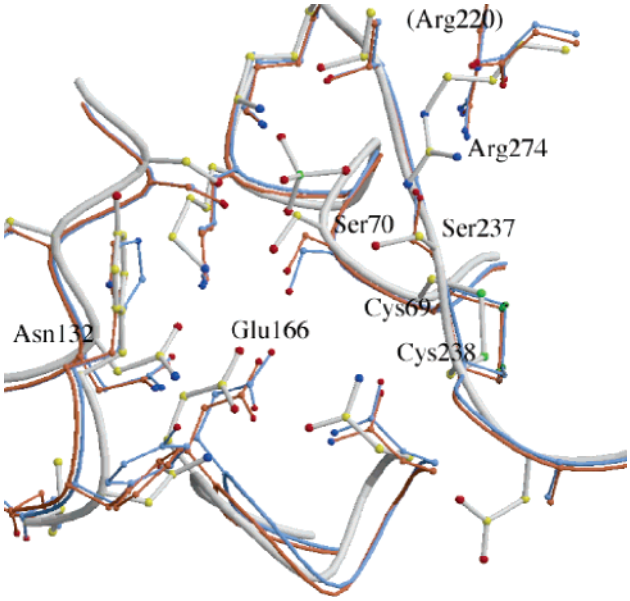

FIGURE 4: Superposition of the G238C structure with carbapenemases Sme-1 and NMC-A structures at the active site. The Toho-1 G238C mutant is coloredwhite, Sme-1 pink, and NMC-A blue. This figure was drawn with O, Molscript, and Raster3D.

would not apply to Toho-1. To understand the importance of β-strand B3 flexibility and the role of Ser237 in Toho-1, further studies, including mutagenic analysis in the vicinity of residue 237, will be required.

It is well-known that the disulfide bond between Cys69 and Cys238 is conserved in several class A carbapenemases (Figure 1), and it has been expected that the introduction of a new disulfide bond might change the kinetic properties of class A β-lactamases, bringing them somewhat closer to those of the carbapenemases (*13*). The X-ray analyses of carbapenem-hydrolyzing class A β-lactamases Sme-1 and NMC-A revealed several unique structural features not observed in other class A enzymes. For example, a shorter distance, and thus direct hydrogen bonding between Ser70 and Glu166, is observed in Sme-1 (*11*). There is a difference in the position of Asn132 in NMC-A, resulting in a wider space for the 6α-hydroxyethyl group of carbapenem and thus making it possible for the NMC-A enzyme to hydrolyze it (*12*). In the case of Toho-1, disulfide bond formation was not confirmed for the G238C/G239in mutant, even though this mutant was designed on the basis of the carbapenemase sequences. This failure seemed to be caused by a difference in the overall protein architecture between Toho-1 and the carbapenemases (*12*). The crystal structure of the G238C mutant, in which the disulfide bond was formed between residues 69 and 238, shows that the disulfide bridge formation in Toho-1 does not cause significant changes in its overall structure as mentioned above, and introduction of the S−S bond itself does not bring the structure of the enzyme any closer to those of the carbapenemases (Figure 4). Moreover, the Toho-1 mutants analyzed in this study did not acquire hydrolytic activity against cabapenem. Thus, our structural and kinetic analyses suggest that the formation of a disulfide bond between Cys69 and Cys238 is not sufficient to confer catalytic activity against carbapenems. The studies of carbapenemase Sme-1 indicated that the disulfide bond between Cys69 and Cys238 was required for the hydrolysis of all the β-lactam antibiotics that were tested, including imipenem (*11*, *39*). Since our study showed no direct correlation between the existence of the disulfide bond and the hydrolytic activity against imipenem, it appears that the disulfide bridge at this position may be important for the structural stability of the class A carbapenemases. Alternatively, we speculate that the disulfide bond in carbapenemases may play a role in clamping of the substrates, including carbapenems, tightly and in an optimal position for hydrolysis, since a decrease in K_m for all of the substrates was observed in the Toho-1 G238C mutant.

ACKNOWLEDGMENT

We thank Professor Noriyoshi Sakabe, Dr. Mamoru Suzuki, Dr. Noriyuki Igarashi, and the entire staff of the Photon Factory, KEK, for their kind help with data collection and data processing. Thanks also go to Dr. Yoshikazu Ishii and Professor Keiko Abe for their support.

REFERENCES

1. Ambler, R. P., Coulson, A. F., Frere, J.-M., Ghuysen, J.-M., Joris, B., Forsman, M., Levesque, R. C., Tiraby, G., and Waley, S. G. (1991) A standard numbering scheme for the class A β-lactamases, *Biochem. J. 276*, 269−270.
2. Helfand, M. S., and Bonomo, R. A. (2003) β-Lactamases: A survey of protein diversity, *Curr. Drug Targets Infect. Disord. 3*, 9−23.
3. Matagne, A., Lamotte-Brasseur, J., and Frere, J.-M. (1998) Catalytic properties of class A β-lactamases: Efficiency and diversity, *Biochem. J. 330*, 581−598.
4. Matagne, A., and Frere, J.-M. (1995) Contribution of mutant analysis to the understanding of enzyme catalysis: The case of class A β-lactamases, *Biochim. Biophys. Acta 1246*, 109−127.
5. Petrosino, J., Cantu, C., III, and Palzkill, T. (1998) β-Lactamases: Protein evolution in real time, *Trends Microbiol. 6*, 323−327.
6. Knox, J. R. (1995) Extended-spectrum and inhibitor-resistant TEM-type β-lactamases: Mutations, specificity, and three-dimensional structure, *Antimicrob. Agents Chemother. 39*, 2593−2601.
7. Tzouvelekis, L. S., Tzelepi, E., Tassios, P. T., and Legakis, N. J. (2000) CTX-M-type β-lactamases: An emerging group of extended-spectrum enzymes, *Int. J. Antimicrob. Agents 14*, 137−142.
8. Ibuka, A., Taguchi, A., Ishiguro, M., Fushinobu, S., Ishii, Y., Kamitori, S., Okuyama, K., Yamaguchi, K., Konno, M., and Matsuzawa, H. (1999) Crystal structure of the E166A mutant of extended-spectrum β-lactamase Toho-1 at 1.8 Å resolution, *J. Mol. Biol. 285*, 2079−2087.
9. Naas, T., Vandel, L., Sougakoff, W., Livermore, D. M., and Nordmann, P. (1994) Cloning and sequence analysis of the gene for a carbapenem-hydrolyzing class A β-lactamase, Sme-1, from *Serratia marcescens* S6, *Antimicrob. Agents Chemother. 38*, 1262−1270.
10. Nordmann, P., Mariotte, S., Naas, T., Labia, R., and Nicolas, M. H. (1993) Biochemical properties of a carbapenem-hydrolyzing β-lactamase from *Enterobacter cloacae* and cloning of the gene into *Escherichia coli*, *Antimicrob. Agents Chemother. 37*, 939−946.
11. Sougakoff, W., L'Hermite, G., Pernot, L., Naas, T., Guillet, V., Nordmann, P., Jarlier, V., and Delettre, J. (2002) Structure of the imipenem-hydrolyzing class A β-lactamase SME-1 from *Serratia marcescens*, *Acta Crystallogr. D58*, 267−274.
12. Swaren, P., Maveyraud, L., Raquet, X., Cabantous, S., Duez, C., Pedelacq, J. D., Mariotte-Boyer, S., Mourey, L., Labia, R., Nicolas-Chanoine, M. H., Nordmann, P., Frere, J.-M., and Samama, J. P. (1998) X-ray analysis of the NMC-A β-lactamase at 1.64-Å resolution, a class A carbapenemase with broad substrate specificity, *J. Biol. Chem. 273*, 26714−26721.
13. Raquet, X., Lamotte-Brasseur, J., Bouillenne, F., and Frere, J. M. (1997) A disulfide bridge near the active site of carbapenem-hydrolyzing class A β-lactamases might explain their unusual substrate profile, *Proteins 27*, 47−58.
14. Ishii, Y., Ohno, A., Taguchi, H., Imajo, S., Ishiguro, M., and Matsuzawa, H. (1995) Cloning and sequence of the gene encoding

a cefotaxime-hydrolyzing class A β-lactamase isolated from *Escherichia coli*, *Antimicrob. Agents Chemother. 39*, 2269−2275.
15. Ibuka, A. S., Ishii, Y., Galleni, M., Ishiguro, M., Yamaguchi, K., Frere, J.-M., Matsuzawa, H., and Sakai H. (2003) Crystal structure of extended-spectrum β-lactamase Toho-1: Insights into the molecular mechanism for catalytic reaction and substrate specificity expansion, *Biochemistry 42*, 10634−10643.
16. Kunkel, T. A., Roberts, J. D., and Zakour, R. A. (1987) Rapid and efficient site-specific mutagenesis without phenotypic selection, *Methods Enzymol. 154*, 367−382.
17. Creighton, T. E. (1989) Disulphide bonds between cysteine residues, in *Protein Structure: A Practical Approach* (Creighton, T. E., Ed.) 1st ed., pp 155−157, IRL Press at Oxford University Press, New York.
18. De Meester, F., Joris, B., Reckinger, G., Bellefroid-Bourguignon, C., Frere, J.-M., and Waley, S.-G. (1987) Automated analysis of enzyme inactivation phenomena. Application to β-lactamases and DD-peptidases, *Biochem. Pharmacol. 36*, 2393−2403.
19. Steller, I., Bolotovsky, R., and Rossmann, M. G. (1997) An algorithm for automatic indexing of oscillation images using Fourier analysis, *J. Appl. Crystallogr. 30*, 1036−1040.
20. Bolotovsky, R., Steller, I., and Rossmann M. G. (1998) The use of partial reflections for scaling and averaging X-ray area-detector data, *J. Appl. Crystallogr. 31*, 708−717.
21. Brunger, A. T., Adams, P. D., Clore, G. M., DeLano, W. L., Gros, P., Grosse-Kunstleve, R. W., Jiang, J. S., Kuszewski, J., Nilges, M., Pannu, N. S., Read, R. J., Rice, L. M., Simonson, T., and Warren, G. L. (1998) Crystallography & NMR system: A new software suite for macromolecular structure determination, *Acta Crystallogr. D54*, 905−921.
22. Jones, T. A., and Kjeldgaard, M. (1995) *Manual for O version 5.10*, Uppsala University, Uppsala, Sweden.
23. Laskowski, R. A., MacArthur, M. W., Moss, D. S., and Thornton, J. M. (1993) PROCHECK: A program to check the stereochemical quality of protein structures, *J. Appl. Crystallogr. 26*, 283−291.
24. Collaborative Computational Project, Number 4 (1994) The CCP4 suite: Programs for protein crystallography, *Acta Crystallogr. D50*, 760−763.
25. Herzberg, O. (1991) Refined crystal structure of β-lactamase from *Staphylococcus aureus* PC1 at 2.0 Å resolution, *J. Mol. Biol. 217*, 701−719.
26. Huletsky, A., Knox, J. R., and Levesque, R. C. (1993) Role of Ser-238 and Lys-240 in the hydrolysis of third-generation cephalosporins by SHV-type β-lactamases probed by site-directed mutagenesis and three-dimensional modeling, *J. Biol. Chem. 268*, 3690−3697.
27. Venkatachalam, K. V., Huang, W., LaRocco, M., and Palzkill, T. (1994) Characterization of TEM-1 β-lactamase mutants from positions 238 to 241 with increased catalytic efficiency for ceftazidime, *J. Biol. Chem. 269*, 23444−23450.
28. Taibi, P., and Mobashery, S. (1995) Mechanism of Turnover of Imipenem by TEM, *J. Am. Chem. Soc. 117*, 7600−7605.
29. Zawadzke, L. E., Smith, T. J., and Herzberg, O (1995) An engineered *Staphylococcus aureus* PC1 β-lactamase that hydrolyses third-generation cephalosporins, *Protein Eng. 8*, 1275−1285.
30. Cantu, C., III, Huang, W., and Palzkill, T. (1996) Selection and characterization of amino acid substitutions at residues 237−240 of TEM-1 β-lactamase with altered substrate specificity for aztreonam and ceftazidime, *J. Biol. Chem. 271*, 22538−22545.
31. Shimamura, T., Ibuka, A., Fushinobu, S., Wakagi, T., Ishiguro, M., Ishii, Y., and Matsuzawa, H. (2002) Acyl-intermediate structures of the extended-spectrum class A β-lactamase, Toho-1, in complex with cefotaxime, cephalothin, and benzylpenicillin, *J. Biol. Chem. 277*, 46601−46608.
32. Tranier, S., Bouthors, A. T., Maveyraud, L., Guillet, V., Sougakoff, W., and Samama, J. P. (2000) The high-resolution crystal structure for class A β-lactamase PER-1 reveals the bases for its increase in breadth of activity, *J. Biol. Chem. 275*, 28075−28082.
33. Knox, J. R., Moews, P. C., and Frere, J. M. (1996) Molecular evolution of bacterial β-lactam resistance, *Chem. Biol. 3*, 937−947.
34. Banerjee, S., Pieper, U., Kapadia, G., Pannell, L. K., and Herzberg, O. (1998) Role of the Ω-loop in the activity, substrate specificity, and structure of class A β-lactamase, *Biochemistry 37*, 3286−3296.
35. Tamaki, M., Nukaga, M., and Sawai, T. (1994) Replacement of serine 237 in class A β-lactamase of *Proteus vulgaris* modifies its unique substrate specificity, *Biochemistry 33*, 10200−10206.
36. Nukaga, M., Mayama, K., Crichlow, G. V., and Knox, J. R. (2002) Structure of an extended-spectrum class A β-lactamase from *Proteus vulgaris* K1, *J. Mol. Biol. 317*, 109−117.
37. Sougakoff, W., Naas, T., Nordmann, P., Collatz, E., and Jarlier, V. (1999) Role of Ser-237 in the substrate specificity of the carbapenem-hydrolyzing class A β-lactamase Sme-1, *Biochim. Biophys. Acta 1433*, 153−158.
38. Gazouli, M., Tzelepi, E., Sidorenko, S. V., and Tzouvelekis, L. S. (1998) Sequence of the gene encoding a plasmid-mediated cefotaxime-hydrolyzing class A β-lactamase (CTX-M-4): Involvement of serine 237 in cephalosporin hydrolysis, *Antimicrob. Agents Chemother. 42*, 1259−1262.
39. Majiduddin, F. K., and Palzkill, T. (2003) Amino acid sequence requirements at residues 69 and 238 for the SME-1 β-lactamase to confer resistance to β-lactam antibiotics, *Antimicrob. Agents Chemother. 47*, 1062−1067.
40. Kraulis, P. J. (1991) MOLSCRIPT: A program to produce both detailed and schematic plots of protein structures, *J. Appl. Crystallogr. 24*, 946−950.
41. Esnouf, R. M. (1997) An extensively modified version of MolScript that includes greatly enhanced coloring capabilities, *J. Mol. Graphics 15*, 132−134.
42. Bacon, D. J., and Anderson, W. F. (1988) A fast algorithm for rendering space-filling molecule pictures, *J. Mol. Graphics 6*, 219−220.
43. Merritt, E. A., and Murphy, M. E. P. (1994) Raster3D version 2.0: A program for photorealistic molecular graphics, *Acta Crystallogr. D50*, 869−873.

BI048488U